
A deep learning and digital archaeology approach for mosquito repellent discovery

Anonymous Author(s)

Affiliation

Address

email

Abstract

1 Insect-borne diseases kill >0.5 million people annually. Currently available re-
2 pellents for personal or household protection are limited in their efficacy, appli-
3 cability, and safety profile. Here, we describe a machine-learning-driven high-
4 throughput method for the discovery of novel repellent molecules. To achieve
5 this, we digitized a large, historic dataset containing 19,000 mosquito repellency
6 measurements. We then trained a graph neural network (GNN) to map molecular
7 structure and repellency. We applied this model to select 317 candidate molecules
8 to test in parallelizable behavioral assays, quantifying repellency in multiple pest
9 species and in follow-up trials with human volunteers. The GNN approach out-
10 performed a chemoinformatic model and produced a hit rate that increased with
11 training data size, suggesting that both model innovation and novel data collection
12 were integral to predictive accuracy. We identified >10 molecules with repellency
13 similar to or greater than the most widely used repellents. This approach enables
14 computational screening of billions of possible molecules to identify empirically
15 tractable numbers of candidate repellents, leading to accelerated progress towards
16 solving a global health challenge.

17 1 Introduction

18 Mosquitos and other blood-sucking arthropods carry and transmit diseases that kill hundreds of thou-
19 sands of people each year Simmons et al. [2012], noa [a]. To make continued progress on this global
20 health issue, we must discover, manufacture, and deploy more efficient molecules for pest control
21 across a variety of application spaces collectively termed vector control; this includes molecules
22 that affect life history traits, such as insecticides, and molecules that affect host-seeking behavior,
23 e.g. topical repellents for personal protection and spatial repellents applied to a home or room.
24 The commonly used repellents DEET (N,N-diethyl-meta-toluamide) and IR3535 (Ethyl butylacety-
25 laminopropionate) are not very potent, and high concentrations must be used in topical applications.
26 Furthermore, they have undesirable properties and/or safety profiles; for example, DEET is a plasti-
27 cizer, precluding its use on synthetic clothing or shelter surfaces, and it is toxic to some vertebrate
28 wildlifenoa [b]. Some commonly used repellents are species-specific; for example IR3535 is ef-
29 fective against *Aedes aegypti* but is ineffective against *Anopheles* mosquitoes and is therefore not
30 recommended for use in malaria-endemic regions. Over the past few decades, only a few dozen new
31 repellent molecule candidates have been found and very few have reached the market; an approach
32 to rapidly discover and validate large numbers of new candidates is desperately needed.

33 Multiple strategies exist for identifying insect repellent candidates. Behavioral assays seek to di-
34 rectly test repellent activity in realistic conditions. Recognizing the devastating effect of insect-borne
35 diseases (including dengue fever) faced by the United States Army during the second world war, the
36 U.S. Department of Agriculture (USDA) tested 30,000 molecules for their effectiveness as repellents

37 and insects on mosquitos, ticks, and other insect speciesFA Morton, BV Travis, JP Linduska [1947],
38 Travis et al. [1949]. In particular, 14,000 molecules were tested for their effectiveness as mosquito
39 (*A. aegypti* and *A. quadrimaculatus*) repellents using human volunteers; this effort led to the discov-
40 ery of DEET. Structure-targeted modeling of the obligatory insect olfactory co-receptor Orco led to
41 discovery of picaridinBoeckh et al. [1996] and VUAA1Jones et al. [2011]. Scaffold-hopping tech-
42 niquesSun et al. [2012] can focus the molecular search space, and in combination with arm-in-cage
43 testing, led to the discovery of IR3535Klier and Kuhlow [1976] and DEPAKalyanasundaram [1982].
44 Chemoreceptor studies exploit the molecular mechanism of action: DEET and IR3535 modulate
45 the activity of G-protein coupled receptors, including odorant and gustatory receptorsDickens and
46 Bohbot [2013], Ditzen et al. [2008] but may also affect cholinergic signalingAbd-Ella et al. [2015],
47 Moreau et al. [2020]. The exact molecular details of their mode of action are not fully understood,
48 and may be very species-specific (Afify and Potter, 2020). It is difficult to more broadly and system-
49 atically explore molecular space using each of these approaches, as they can be labor-intensive.

50 The USDA dataset represents a wealth of information on the relationship between molecular struc-
51 ture and arthropod behavior. Small parts of this dataset have been used previously to train compu-
52 tational models of mosquito repellencyWright [1956], Katritzky et al. [2008], Bernier and Tsikolia
53 [2011], typically on specific structural families of molecules. Katritzky et al.Katritzky et al. [2010]
54 used an artificial neural network model trained on 167 carboxamides and found 1 carboxamide can-
55 didate with high repellency activity. As modern deep learning models show performance which
56 scales in proportion to the volume of their training dataGwern, we hypothesized that exploiting
57 the full size of the USDA dataset would provide a strong starting point for a new deep learning
58 model. We selected a graph neural network architecture (GNN), as GNNs have been shown to have
59 superior performance to computable chemoinformatics descriptors in predicting the properties of a
60 molecule from its chemical structure, given a sufficiently large datasetWu et al. [2018], Duvenaud
61 et al. [2015a]. Notably, previous work demonstrated that a GNN-based human odor model outper-
62 forms standard cheminformatics models even on insect behavior datasets.Wright [1956], Katritzky
63 et al. [2008], Bernier and Tsikolia [2011]

64 Here we present a data-driven workflow for the discovery and validation of novel molecules for
65 behavioral modification in arthropods. The critical components underlying the success of this ap-
66 proach are 1) expanded training data made possible by a complete digitization of the USDA dataset;
67 2) high-quality validation data using a parallelizable membrane-feeding assay that does not require
68 human volunteers; and 3) a graph neural network model to learn the relationship between molecular
69 structure and these data. We iteratively use this model to propose candidates from a purchasable
70 chemical library, validate these candidates for repellency, and use these results to expand the train-
71 ing dataset and therefore improve the predictive accuracy of the behavior model (Figure 1). Through
72 this process we have discovered a chemically diverse set of molecules with effectiveness equal to or
73 greater than DEET, unlocking new potential capabilities in vector control.

74 2 Results

75 2.1 Digitizing a rich historical dataset

76 The USDA dataset is unmatched in size and scope, but for decades existed only in print. Google
77 Books scanned and made available the original work onlineFA Morton, BV Travis, JP Linduska
78 [1947], and for this work we subsequently converted it into a machine-readable format. After some
79 preprocessing to make the dataset easier to read, we employed expert curators to transcribe the full
80 records and provide canonical structures for each listed molecule (Fig. 2A, Methods). We then
81 focused our analysis on the four mosquito repellency assays contained in this dataset: two mosquito
82 species, *Aedes aegypti* and *Anopheles quadrimaculatus*; and two repellency contexts, skin and cloth.
83 Together these comprise 19,000 labeled data points on repellency of specific molecules (Fig. 2B),
84 representing a broad range of structural and functional classes (Fig. 2C). This large dataset served
85 as training data for our modeling efforts.

86 2.2 Assessment of repellent candidates

87 In order to test model predictions and iteratively expand the training data, we adapted a standard
88 membrane feeding assay (SMFA), commonly used in malaria researchBoyd [1949], Churcher et al.
89 [2012], to evaluate the repellency against *Anopheles stephensi* mosquitoes. Repellency was eval-

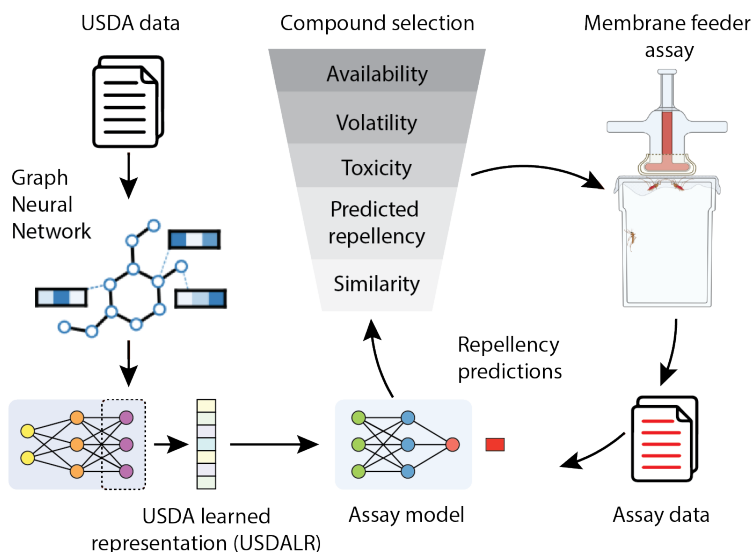


Figure 1: **Pipeline for active learning of new behavior repellent molecules.** A large historical dataset from the USDA (USDA data) was used to train a graph neural network to generate a fixed vector representation of any candidate molecule (USDA learned representation, USDALR). To create the transfer-learned assay model, molecules are first embedded with the USDA learned representation and fed to a dense neural network; this assay model is trained on the assay data. A large-scale in silico molecular screen is applied to select candidate molecules for testing in a membrane feeder assay for repellency. Resulting data are used to train the assay model. In subsequent iterations, the assay results are used to improve the transfer-learning model, a form of active learning.

90 uated by prevention of blood feeding relative to a vehicle (ethanol) control (Fig. 2D). The assay
 91 was used to evaluate each molecules potency and duration of effect as exemplified for the reference
 92 molecule DEET in Fig 2E. We assessed the inherent inter-assay reliability by comparing repellency
 93 levels for a diverse set of molecules from independent experiments (tested at 25 $\mu\text{g}/\text{cm}^2$, $r=0.81$, Fig.
 94 2F). Using a cut-off of 75% repellency as measured 120 min after initial application, selected to
 95 include widely used repellents (e.g. DEET, dimethyl phthalate, and indalone), approximately 3/4 of
 96 the molecules classified as active in a first assay were confirmed to be active upon re-testing.

97 The USDA dataset was collected 70 years ago using arm-in-cage experiments, involving human
 98 volunteers, while our assay was conducted with a surrogate target. We evaluated the relationship
 99 between these two experiments by directly comparing the activity of 38 molecules with their repel-
 100 lency reported in the USDA dataset. We found considerable concordance between the historical
 101 USDA dataset and the membrane feeding assays ($p<0.01$ Mann Whitney U test, Fig. 2G), despite
 102 differences in experimental setup. However, some disagreement was observed, highlighting the need
 103 for additional data collection.

104 2.3 Modeling mosquito repellency behavior

105 Using the USDA dataset, we sought to create a representation of molecules specific to mosquito
 106 repellency behavior. It has been previously demonstrated that graph neural networks (GNNs) are
 107 particularly adept at creating task-specific representations Duvenaud et al. [2015b], Wu et al. [2018],
 108 and that representational power extends to the domain of olfaction Sanchez-Lengeling et al. [2019],
 109 Qian et al. [2022]. We trained GNN models on the USDA dataset, observing an AUC=0.881 on
 110 the cloth-*Aedes aegypti* task, the task with the largest dataset (Methods). We then use the output
 111 heads from the ensemble models on all four USDA tasks to create the USDA learned representation
 112 (USDALR, Figure 1).

113 We sought to build a model that was specific for the activity behavior in our membrane feeder assay.
 114 We created an assay model by first using the fixed USDA learned representation to embed input
 115 molecules, then adding a two layer, 256-node neural network to learn to predict the assay data.

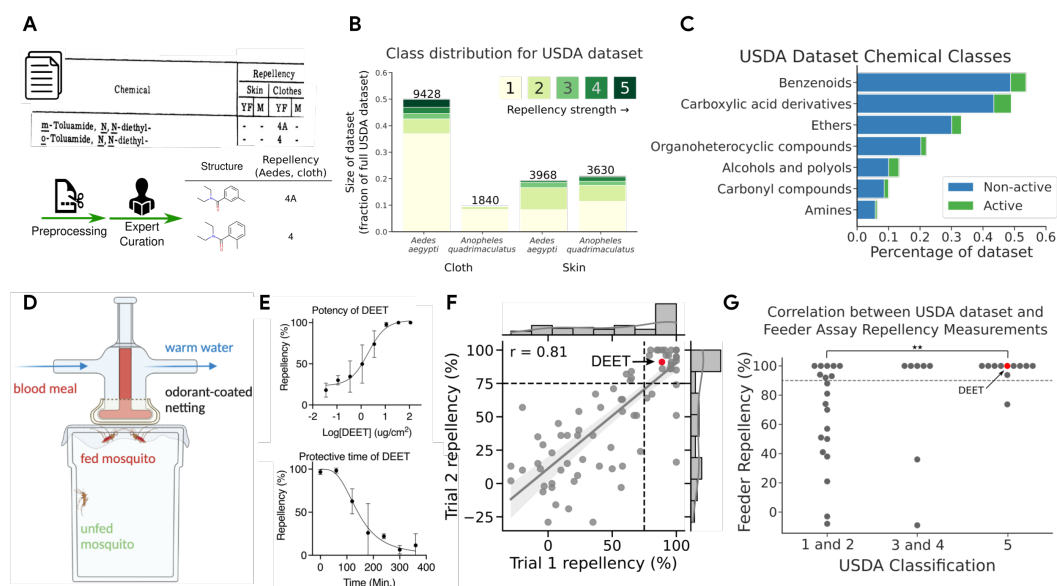


Figure 2: Overview of data sources. (A) The USDA dataset scanned into Google Books was digitized and manually curated into a machine-readable table of repellency ratings for each compound (King, WV 1954). (B) Digitized ratings from USDA dataset used here covered two assay types and two mosquito species. (C) The USDA dataset covered a diverse range of chemical classes; shown here is the distribution of some ClassyFire classes (Djoumbou-Feunang et al. 2016). Active compounds are defined as class 4 or higher. (D) Our validation assay used warmed blood and an odorant-coated netting; repellency was identified with a decrease in feeding behavior relative to a control odorant (ethanol). (E) Repellency measured using the assay in (D); 100% indicates total repellency (no feeding) and 0% matches behavior using the solvent alone. Data points (mean \pm SD across replicates) show repellency using the indicated concentration of DEET as the odorant. Top: Repellency of DEET at $t=120$ min. increases with concentration. Bottom: Repellency decreases with time after initial application of the odorant (sigmoidal fit). (F) Repellency values are correlated across independent replications of the assay. Trials 1 and 2 are not necessarily in chronological order. Test-retest values of DEET are indicated in red. Dotted line indicates positive activity cutoff at Repellency=0.75 for $t=120$ min. (G) Repellency observed in the assay at $t=2$ min. at 1% concentration using *A. stephensi* is concordant with repellency from the USDA dataset using *A. aegypti* on cloth. Dotted line represents activity cutoff at Repellency=0.9 for $t=2$ min. for feeder assay. DEET's activity is represented by a red dot. Raw repellency % for USDA Class 1&2 vs Class 5: $p<0.01$ (Mann-Whitney U Test); Hit percentage: $p<0.05$ (Z-test of proportions).

116 We applied the assay model to make predictions on novel repellent candidate compounds from
 117 a large library of purchasable molecules provided by the vendor eMoleculesMolecules. We fil-
 118 tered this library for desirable qualities such as volatility and low cost, and we further screened out
 119 molecules which did not pass an inhalation toxicity filter (Methods). From among those compounds
 120 passing these filters (10k molecules), we selected those which had sufficient predicted repellency
 121 and—to ensure novelty—which were structurally distinct (Tanimoto similarity <0.8) from those in the
 122 USDA dataset or previous candidate selections. Assay results from each batch of selections were
 123 added to the assay dataset; for each subsequent batch of selections, the assay model was re-trained
 124 on the expanded assay dataset. Detailed notes on the specific modeling setup for each batch are
 125 located in the Supplementary section.

126 Over several iterations, a total of 400 molecules were purchased and further screened empirically
 127 according to a solubility criterion (Methods); those that passed ($n=317$) were then tested for repel-
 128 lency with the membrane-feeder assay. Over the course of selections spanning over a year, some
 129 adjustments were made to both the USDA model and the membrane-feeder assay. In particular,
 130 our hit definition evolved with our dataset size and model capability: we initially defined a hit as
 131 90% repellency using a dose of 25 $\mu\text{g}/\text{cm}^2$ as measured at $T=2$ min (1 measurement), but in the fi-

132 nal batch of selections, we changed our definition to 75% repellency as measured at T=120min (3
133 measurements).

134 **2.4 The hit rate improves with training data size**

135 To evaluate the contribution of the training data to our performance, we retrospectively scored
136 high-repellency candidates in two phases: before the USDA dataset was available (pre-USDA)
137 and after we began using the USDA dataset to build and deploy the USDA learned representation
138 (post-USDA). In the pre-USDA phase, instead of using the USDA learned representation to em-
139 bed molecules, we employed an odor-specific representation previously demonstrated to outperform
140 standard cheminformatics representations on olfaction related tasksQian et al. [2022]. Further, at
141 that time, we only had assay data for 34 molecules, so we opted to use a k-nearest neighbors model
142 (k=10) to model assay activity. In the post-USDA phase, the assay dataset size for the first batch was
143 142 molecules, and grew to a size of 402 molecules for our final batch of selections (Supplemental
144 Batch Notes).

145 This large dataset made a huge difference; hit rates post-USDA measured on repellency time=2min
146 increased to 49% from the pre-USDA level of only 29% (Figure 3A). When we then raised the bar
147 for hit classification to require a longer duration of effect, hit rates dropped to 6% for predictions
148 from the post-USDA phase and 3% for predictions from the pre-USDA phase. It is important to
149 note that only the last batch in the post-USDA phase was trained to find candidates meeting this new
150 repellent standard; further iterations may have continued to improve performance as they did under
151 the previous standard.

152 This hit rate comparison across the two different experimental phases aggregates changes in both
153 representational approach and assay dataset size; how much did the USDA learned representation
154 specifically, and by extension the USDA dataset, improve our models performance?

155 To estimate the contributions of the USDA representation, we performed a retrospective analysis
156 comparing the USDA representation against two other chemical representation approaches: a chem-
157 informatics representation (using Mordred descriptorsMoriwaki et al. [2018]) and the odor-based
158 representationQian et al. [2022] used in the pre-USDA phase. We split the full assay dataset into
159 two parts, a training set composed of molecules from all batches of tests performed before the use
160 of the USDA dataset (88 measurements) and an evaluation set of all molecules selected in the post-
161 USDA phase (170 measurements).

162 We observed that the USDA learned representation model significantly outperformed both alterna-
163 tives on this prediction task (Figure 3B; USDA model AUC=0.74 [0.68,0.81]; Chemoinformatics
164 model AUC=0.59 [0.50,0.67]; GNN Odor model AUC=0.60 [0.51,0.67]), suggesting that the histor-
165 ical dataset played a significant role in the elevated predictive performance. There is a selection bias
166 because the selection of molecules for evaluation was done by the assay model using USDA learned
167 representations. One effect of this bias is that it reduces the expected number of negative exam-
168 ples, reducing the contrast between predicted repellents and non-repellents, resulting in a negative
169 bias into all AUC measurements. However, the model used for selection should suffer the greatest
170 negative bias, suggesting that the performance difference we observed is an underestimate of the
171 true advantage that the USDA model has over its alternatives, as would have been observed under a
172 counterfactual unbiased selection of repellent candidates.

173 **2.5 Selected hit molecules are chemically diverse**

174 Training a model on a large pool of data containing a variety of molecules allows the model to
175 generalize to larger areas of chemical space. Figure 4 shows the distribution of molecules selected
176 by our post-USDA models, and compares them to the active molecules reported in the USDA dataset
177 itself. The candidate selections made by our model explore some of the same regions of the USDA
178 dataset, but find hits in some underexplored regions of the original dataset (Figure 4A). The ML-
179 selected molecules were required to be a minimum of 0.2 Tanimoto distance from USDA molecules;
180 we observe an overall median Tanimoto distance of 0.52 from USDA molecules across all of our
181 selections, and a median distance of 0.48 from USDA molecules amongst active molecules (Figure
182 4B). Using ClassyFireDjoumbou Feunang et al. [2016] to annotate each molecule, we found that
183 molecules selected by our model are enriched in benzenoids, ethers, carboxylic acid derivatives,

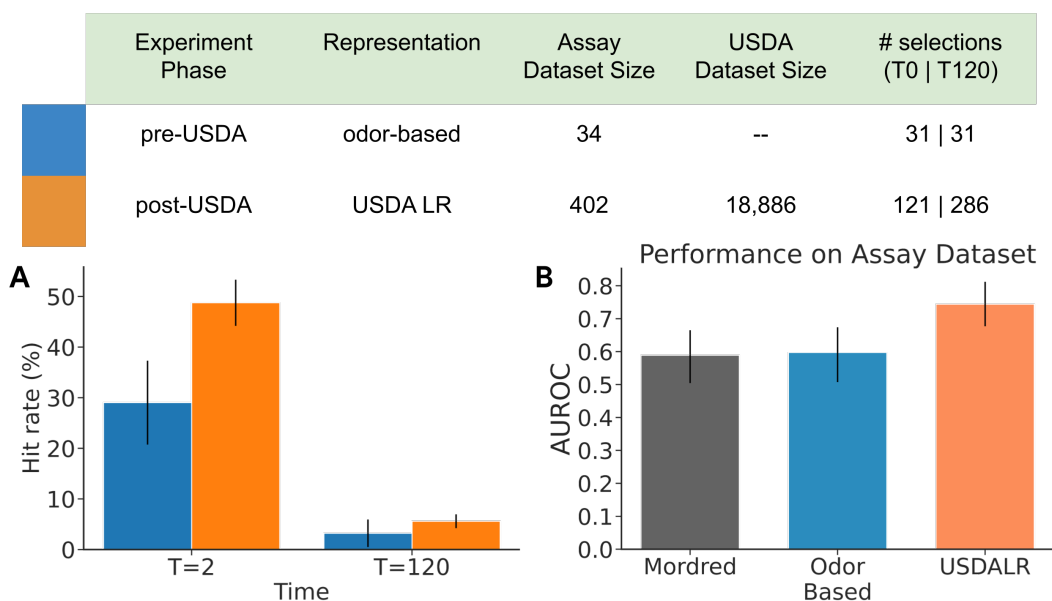


Figure 3: **The table reflects experimental testing set up in pre-USDA phase, i.e. before the use of the USDA dataset for modeling, and post-USDA phase, i.e. after the use of the USDA dataset.** (A) Active repellent compounds found at a much higher rate in post-USDA phase (49%) vs. pre-USDA phase (29%). Hits are defined as compounds that showed >90% repellency in the feeder assay at initial application (t=2 min) or >75% repellency after 2 hours of evaporation (t=120). Error bars represent the standard error of jackknife estimated mean values. (B) In a retrospective prediction task, USDA learned representation model (USDALR) outperforms models using cheminformatics representation (Mordred, Moriwaki et al, 2018) and odor-based representation (Qian et al. 2022). Models were trained on assay data collected before USDA modeling (88 data points), and evaluated on post-USDA measurements (170 data points). Error bars represent 95% bootstrap-resampling confidence intervals.

184 and organoheterocyclic molecules when compared to the molecules measured by the USDA dataset
 185 (Figure 4C).

186 2.6 Top candidates show strong repellency in additional applications

187 While the membrane feeder assay provides a rapid measurement of repellency effectiveness, for real-
 188 world applications it is necessary to consider the effect of odorants released by human skin. To assess
 189 repellency of hit molecules in the context of host skin emanations, we tested a representative set of
 190 our molecules in arm-by-cage experiments (Fig. 5A). To this end, we selected 31 hit molecules that
 191 showed 75% repellency at a density of 25 $\mu\text{g}/\text{cm}^2$ at T=120 minutes at least once in the membrane
 192 feeder experiments, and 4 molecules with lower repellency activities. When tested at a density of
 193 13 $\mu\text{g}/\text{cm}^2$ in the arm-by-cage experiments, 43% of the tested molecules perform very well (75%
 194 repellency) and 67% of those even outperform DEET (>84% repellency) (Fig. 5B). Overall, we
 195 observed high correspondence between repellency as measured in the feeder vs. the arm-in-cage
 196 assays ($r=0.64$), with 83% of hits from the former also reaching the hit threshold in the latter (Fig.
 197 5C).

198 Our primary assay assessed repellency against *A. stephensi*, but other pest species also carry dis-
 199 ease, and there are some known species-specific differences in repellency of known molecules
 200 (e.g. IR3535). To address this concern, we selected 16 molecules based on their activity against
 201 *A. stephensi*, 9 strong and 7 weak repellents. We then used the original assay to test them against
 202 *A. aegypti* and a modified assay (Fig. 5D) to test against *I. scapularis*, the black-legged tick. We ob-
 203 served significant generalization across pest species: 8 of the strong repellents (88%) demonstrated

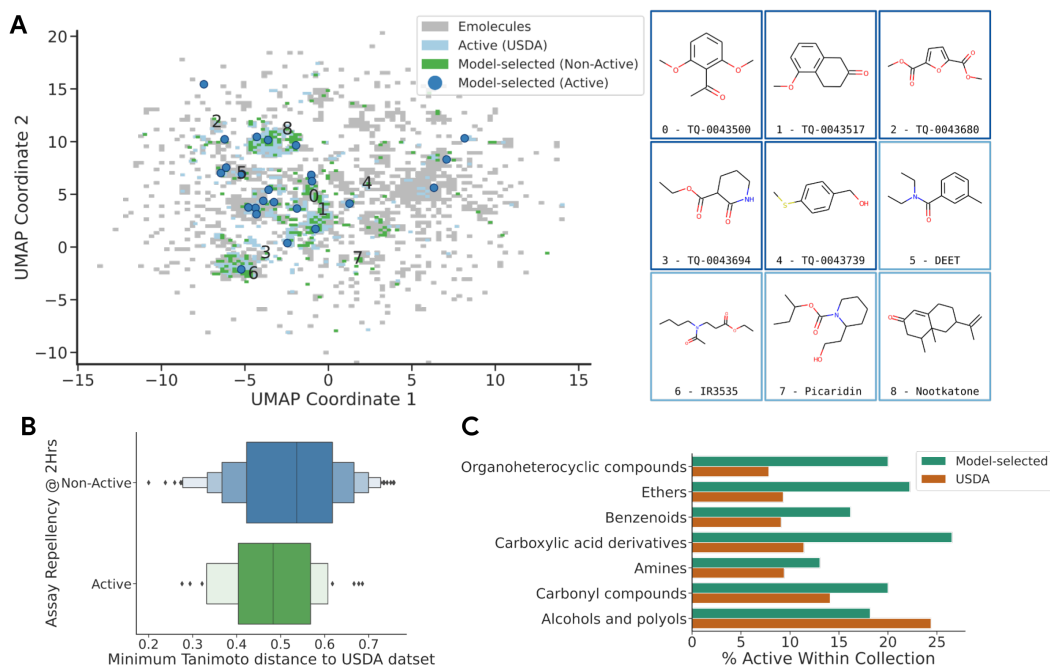


Figure 4: **Analysis of the chemical space we explored.** (A) The model-selected molecules are distributed throughout the chemical space, with some active molecules found both near and far from USDA clusters. Shown is a UMAP embedding of USDA active molecules (light blue), and model selected molecules (dark blue), aligned with the eMolecules library (grey heatmap), using Morgan fingerprint features ($r=4$, $n=2048$). The positions of a few high-repency, model-selected compounds and several known repellents are shown. (B) Tanimoto distance of ML-selected candidates to the USDA dataset; molecules were selected to be at least Tanimoto distance=0.2 away from other USDA molecules, with active candidates having a lower median distance away from the USDA dataset (median=0.48) compared to inactive candidates (median=0.54). (C) Distribution of ClassyFire classes (Djoumbou-Feunang et al., 2016) in the USDA dataset and the TropIQ selections. TropIQ selections are enriched for organoheterocyclic compounds, ethers, benzenoids, and carboxylic acid derivatives.

204 good repellency (>50% repellency) at 25 $\mu\text{g}/\text{cm}^2$ against *A. aegypti*, and 12 (75%) molecules were
 205 active (>75% repellency) at 540 $\mu\text{g}/\text{cm}^2$ against *I. scapularis* (ED50 of DEET 120 $\mu\text{g}/\text{cm}^2$, Fig. 5E).

206 3 Discussion

207 We developed and validated novel methods for identifying potential repellent molecules for vector
 208 control of deadly human and animal diseases. First, we digitized a historic dataset rich with an
 209 unprecedented volume of relevant repellency data covering thousands of molecules. Second, we
 210 applied and refined a deep learning model architecture to learn the mapping between molecular
 211 structure and repellency in this dataset. Third, we used a high-throughput experimental assay to
 212 prospectively validate predictions from this model, and to conduct active learning to iteratively im-
 213 prove model predictions. Finally, we showed that these predictions identify new repellent candidates
 214 in underexplored regions of chemical space, and that some of these molecules show applicability
 215 across real-life context and across pest species. This represents a promising approach to identify
 216 next-generation repellents and help solve one of humanity's greatest global health challenges.

217 Despite containing a surprisingly large quantity of relevant repellency data, the USDA dataset has
 218 remained underused, garnering only 200 citations in the last 50 years. This surely stemmed in
 219 part from the limited visibility and accessibility of the data during most of this period, where it was
 220 accessible only via paper handbooks in physical libraries. The Google Books digitization project

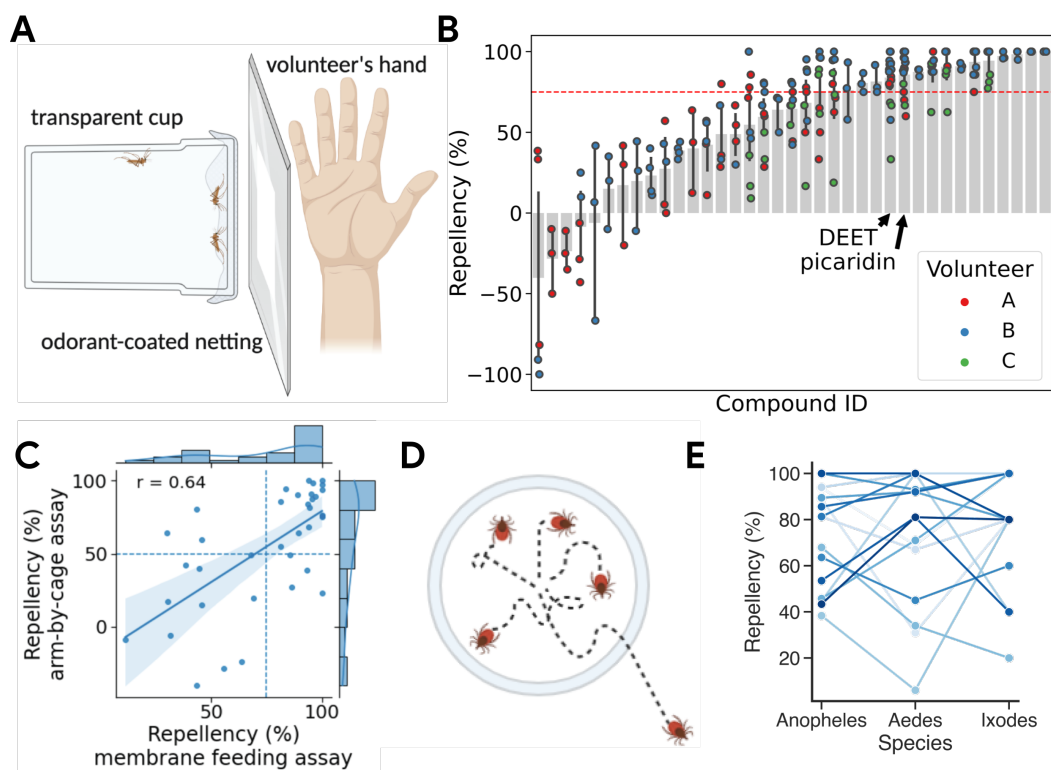


Figure 5: **Model-selected and feeder assay validated compounds show high performance across context and species.** (A) Experimental setup of arm-by-cage experiments on *Anopheles stephensi*. (B) Arm-by-cage repellency of molecules previously determined to be repellent in the membrane feeder assay. (C) Activities of repellents identified in the membrane feeding assay correlate well with the activity in arm-by-cage assays. (D) Experimental setup of *Ixodes scapularis* (tick) repellency assay. Ticks are placed in a repellent-impregnated ring on a heated bed and the number of ticks that cross the ring are counted. (E) Repellency of molecules is correlated across species; one line corresponds to one compound.

221 scanned these handbooks, making images of the data visible to anyone with an internet connection.
 222 However, many of the chemical names contained there-in were archaic or ambiguous, and so could
 223 not be effortlessly mapped to chemical structures; the repellency values themselves were also not
 224 machine readable. The manual curation and digitization that we performed was the last step to
 225 unlock the power of these historical records. The general pattern of connecting diffuse experimental
 226 records to support larger modeling efforts and meta-analyses continues to bear fruit^{30,31}.

227 How important were these data? Machine learning is data-driven, and frequently suffers from cold
 228 start problems; deep learning models are especially data-hungry, and finding enough data to train
 229 them to state-of-the-art performance can be a major challenge. The USDA dataset solved this prob-
 230 lem by allowing us to train a draft model, which we were then able to build upon using data from
 231 a modern experimental assay. Several previous efforts to identify new repellents using machine
 232 learning have used only several dozen similar molecules to train their models^{1517,32}. A larger slice
 233 of the historical dataset (2000 molecules) has been used to train a neural network model to both
 234 predict repellency and verify the repellency of known repellents³³. Recently, larger datasets are
 235 becoming available for receptor-targeted QSAR (RT-QSAR)^{34,35}, but until this current work, no
 236 machine-readable large-scale datasets have been available for BT-QSAR.

237 Most previous publications validated their repellency models only retrospectively by predicting
 238 the activity of known repellents, rather than prospectively³⁶ by using the model to identify new
 239 molecules with repellency behavior. This typically leads to overestimation of predictive perfor-
 240 mance of new repellent candidates. By contrast, we collected assay data for prospective validation

241 of the model, and further used this data in an active learning loop to refine the model, showing
242 continued improvement in predictive performance as new data was collected.

243 Prospective validation has been used in the past to discover new repellent molecules: Picaridin was
244 discovered at Bayer using pharmacophore modeling⁶, and a small set of acylpiperdines were dis-
245 covered using neural networks trained on a small subset of USDA data¹⁷. However, these novel re-
246 pellents have typically been structural near-neighbors of existing repellents. By contrast, our model-
247 selected candidates cover a much wider range of structural classes than previous repellency discov-
248 ery attempts, facilitating our discovery of molecules with repellency activity greater than DEET even
249 at 2 hours after application, and a subset that have repellency efficacy when tested in the presence of
250 attractive human skin emanations.

251 Machine learning, and particularly deep learning, is yielding impressive advances in applications in
252 chemistry. Several academic and industrial groups have used deep learning models to screen for new
253 molecules with desirable properties, such as antibiotic activity or protein binding affinity^{34,3739}.
254 The methods outlined in this paper can also be applied to other disease vectors, other classes of
255 behavior-modifying molecules, and more broadly to enable hit discovery in arbitrary chemical ap-
256 plications. Future work will be required to impose additional filters or modeling steps to satisfy
257 additional criteria related to safety, biodegradability, odor, and skin-feel, in conjunction with experi-
258 mental data about these important factors.

259 References

- 260 Cameron P Simmons, Jeremy J Farrar, van Vinh Chau Nguyen, and Bridget Wills. Dengue. *N. Engl.*
261 *J. Med.*, 366(15):1423–1432, April 2012.
- 262 Vector-borne diseases. [https://www.who.int/news-room/fact-sheets/detail/
263 vector-borne-diseases](https://www.who.int/news-room/fact-sheets/detail/vector-borne-diseases), a. Accessed: 2022-8-26.
- 264 DEET. <http://npic.orst.edu/factsheets/archive/DEETtech.html>, b. Accessed: 2022-
265 8-17.
- 266 FA Morton, BV Travis, JP Linduska. *Results of screening tests with materials evaluated as insecti-*
267 *cides, miticides and repellents at the Orlando, Fla., laboratory : April 1942 to April 1947.* US
268 Department of Agriculture, Bureau of Entomology and Plant Quarantine, 1947.
- 269 Travis, Morton, Jones, and others. The more effective mosquito repellents tested at the orlando, fla.,
270 laboratory, 1942–47. *J. Econ. Financ. Stud.*, 1949.
- 271 Jürgen Boeckh, Heinz Breer, Martin Geier, Franz-Peter Hoever, Bernd-Wieland Krüger, Günther
272 Nentwig, and Hinrich Sass. Acylated 1,3-aminopropanols as repellents against bloodsucking
273 arthropods. *Pestic. Sci.*, 48(4):359–373, December 1996.
- 274 Patrick L Jones, Gregory M Pask, David C Rinker, and Laurence J Zwiebel. Functional agonism of
275 insect odorant receptor ion channels. *Proc. Natl. Acad. Sci. U. S. A.*, 108(21):8821–8825, May
276 2011.
- 277 Hongmao Sun, Gregory Tawa, and Anders Wallqvist. Classification of scaffold-hopping approaches.
278 *Drug Discov. Today*, 17(7-8):310–324, April 2012.
- 279 Klier and Kuhlow. Neue Insektenabwehrmittel—Am stickstoff disubstituierte beta-alaninderivate.
280 *J. Soc. Cosmet. Chem.*, 1976.
- 281 M Kalyanasundaram. A preliminary report on the synthesis and testing of mosquito repellents.
282 *Indian J. Med. Res.*, 76:190–194, July 1982.
- 283 Joseph C Dickens and Jonathan D Bohbot. Mini review: Mode of action of mosquito repellents.
284 *Pestic. Biochem. Physiol.*, 106(3):149–155, July 2013.
- 285 Mathias Ditzen, Maurizio Pellegrino, and Leslie B Vosshall. Insect odorant receptors are molecular
286 targets of the insect repellent DEET. *Science*, 319(5871):1838–1842, March 2008.
- 287 Aly Abd-Ella, Maria Stankiewicz, Karolina Mikulska, Wieslaw Nowak, Cédric Pennetier, Mathilde
288 Goulu, Carole Fruchart-Gaillard, Patricia Licznar, Véronique Apaire-Marchais, Olivier List, Vin-
289 cent Corbel, Denis Servent, and Bruno Lapied. The repellent DEET potentiates carbamate effects
290 via insect muscarinic receptor interactions: An alternative strategy to control insect Vector-Borne
291 diseases. *PLoS One*, 10(5):e0126406, May 2015.
- 292 Eléonore Moreau, Karolina Mikulska-Ruminska, Mathilde Goulu, Stéphane Perrier, Caroline De-
293 shayes, Maria Stankiewicz, Véronique Apaire-Marchais, Wieslaw Nowak, and Bruno Lapied.
294 Orthosteric muscarinic receptor activation by the insect repellent IR3535 opens new prospects in
295 insecticide-based vector control. *Sci. Rep.*, 10(1):6842, April 2020.
- 296 R H Wright. Physical basis of insect repellency. *Nature*, 178(4534):638, September 1956.
- 297 Alan R Katritzky, Zuoquan Wang, Svetoslav Slavov, Maia Tsikolia, Dimitar Dobchev, Novruz G
298 Akhmedov, C Dennis Hall, Ulrich R Bernier, Gary G Clark, and Kenneth J Linthicum. Synthesis
299 and bioassay of improved mosquito repellents predicted from chemical structure. *Proc. Natl.*
300 *Acad. Sci. U. S. A.*, 105(21):7359–7364, May 2008.
- 301 Ulrich R Bernier and Maia Tsikolia. Development of novel repellents using StructureActivity mod-
302 eling of compounds in the USDA archival database. In *Recent Developments in Invertebrate*
303 *Repellents*, volume 1090 of *ACS Symposium Series*, pages 21–46. American Chemical Society,
304 January 2011.

- 305 Alan R Katritzky, Zuoquan Wang, Svetoslav Slavov, Dimitar A Dobchev, C Dennis Hall, Maia
306 Tsikolia, Ulrich R Bernier, Natasha M Elejalde, Gary G Clark, and Kenneth J Linthicum. Novel
307 carboxamides as potential mosquito repellents, 2010.
- 308 Gwern. The scaling hypothesis. <https://www.gwern.net/Scaling-hypothesis>.
- 309 Zhenqin Wu, Bharath Ramsundar, Evan N Feinberg, Joseph Gomes, Caleb Geniesse, Aneesh S
310 Pappu, Karl Leswing, and Vijay Pande. MoleculeNet: a benchmark for molecular machine learn-
311 ing. *Chem. Sci.*, 9(2):513–530, January 2018.
- 312 David K Duvenaud, Dougal Maclaurin, Jorge Iparraguirre, Rafael Bombarell, Timothy Hirzel, Alan
313 Aspuru-Guzik, and Ryan P Adams. Advances in neural information processing systems 28.
314 *Cortes C. , Lawrence ND, Lee DD, Sugiyama M. , Garnett R. , Eds*, pages 2224–2232, 2015a.
- 315 Boyd. Epidemiology: factors related to the definitive host. *Malariaology*, 1949.
- 316 Thomas S Churcher, Andrew M Blagborough, Michael Delves, Chandra Ramakrishnan, Melissa C
317 Kapulu, Andrew R Williams, Sumi Biswas, Dari F Da, Anna Cohuet, and Robert E Sinden. Mea-
318 suring the blockade of malaria transmission—an analysis of the standard membrane feeding assay.
319 *Int. J. Parasitol.*, 42(11):1037–1044, October 2012.
- 320 David Duvenaud, Dougal Maclaurin, Jorge Aguilera-Iparraguirre, Rafael Gómez-Bombarelli, Tim-
321 othy Hirzel, Alán Aspuru-Guzik, and Ryan P Adams. Convolutional networks on graphs for
322 learning molecular fingerprints. *arXiv [cs.LG]*, September 2015b.
- 323 B Sanchez-Lengeling, J N Wei, B K Lee, and others. Machine learning for scent: Learning general-
324 izable perceptual representations of small molecules. *arXiv preprint arXiv*, 2019.
- 325 Wesley W Qian, Jennifer N Wei, Benjamin Sanchez-Lengeling, Brian K Lee, Yunan Luo, Marnix
326 Vlot, Koen Dechering, Jian Peng, Richard C Gerkin, and Alexander B Wiltschko. Metabolic
327 activity organizes olfactory representations. August 2022.
- 328 eMolecules. emolecules. <https://www.emolecules.com/>. Accessed: 2022-8-22.
- 329 Hiroto Moriwaki, Yu-Shi Tian, Norihito Kawashita, and Tatsuya Takagi. Mordred: a molecular
330 descriptor calculator. *J. Cheminform.*, 10(1):4, February 2018.
- 331 Yannick Djoumbou Feunang, Roman Eisner, Craig Knox, Leonid Chepelev, Janna Hastings, Gareth
332 Owen, Eoin Fahy, Christoph Steinbeck, Shankar Subramanian, Evan Bolton, Russell Greiner, and
333 David S Wishart. ClassyFire: automated chemical classification with a comprehensive, com-
334 putable taxonomy. *J. Cheminform.*, 8:61, November 2016.

335 A Method

336 A.1 Mosquitoes and ticks

337 Both *Anopheles stephensi* and *Aedes aegypti* mosquitoes were maintained on a 5% sugar solution
338 in a 26 °C environment with 80% humidity, according to standard rearing procedures. Adult *Ixodes*
339 *scapularis* ticks were maintained in a 26 °C environment with 90% humidity. Mosquito behavioral
340 assays Before each membrane feeding assay, 10-20 female *Anopheles stephensi* or *Aedes aegypti*
341 mosquitoes (3-5 days old) were transferred to a paper cup covered with mosquito netting. The
342 mosquitoes were denied access to their normal sugar solution 4-6 hours prior to the feeding assay.
343 30 μ l of test molecule, dissolved in ethanol, was pipetted on a piece of mosquito netting (3x3 cm)
344 and allowed to dry. To ensure a regular and standardized airflow over the samples, a gastronorm
345 tray (\varnothing 200mm) equipped with a computer fan (80x80x25mm, 12V, 0.08A) was placed over the
346 samples. After a specified time of evaporation (e.g., 2 hours), the sample was placed on top of the
347 cup containing the mosquitoes. The cups were then placed under a row of glass membrane feeders
348 containing a pre-warmed (37 °C) blood meal. The mosquitoes were allowed to feed for 15 minutes.
349 The number of fed and unfed mosquitoes were then recorded.

350 For the arm-by-cage assays, 30-50 female *Anopheles stephensi* mosquitoes were transferred to an
351 acrylic cup (150x100mm) covered with mosquito netting. 1 mL of test molecule (0.5% w/v), dis-
352 solved in ethanol, was pipetted on a piece of cheesecloth (6x9 cm) and taped to an acrylic panel

353 (6mm thick) with a cutout and allowed to dry. A panel with an untreated piece of cloth was then
354 placed next to the acrylic cups containing the mosquitoes and a volunteer placed his hand against the
355 panel for 5 minutes. The mosquitoes were filmed and the maximum number of mosquitoes landing
356 simultaneously was recorded. This was then repeated with a piece of treated cloth and the number of
357 landings was normalized to the control, which is the ethanol solvent alone. All arm-by-cage assays
358 were designed and run by TropIQ.

359 **A.2 Tick behavioral assays**

360 The setup of the tick repellency assay is shown in figure 5D. The assay consists of a heated (37°C)
361 aluminum plate (235 x 235 mm) that is painted white. Before the test, 750 μ l of test molecule,
362 dissolved in ethanol, is pipetted on a ring of filter paper (OD = 150 mm, ID = 122 mm). The ring
363 is then transferred onto the heated plate and 5 *Ixodes scapularis* ticks are placed in the center. The
364 ticks are monitored for 5 minutes and the number of ticks that cross the filter paper are counted.
365 Repellency is expressed as the percentage of ticks that did not cross the filter paper.

366 **A.3 Historical dataset preparation**

367 The scanned versions of the USDA datasets, available from Google Books, were converted into a
368 machine-readable format. Chemical structures (Simplified Molecular-Input Line-Entry System, or
369 SMILES) 40 were assigned to each single molecule entry in the dataset. The raw PDFs of the two
370 repellency handbooks^{41,42} used to create the USDA dataset are available on Google Books. For
371 this study, the PDFs were converted to png files, then sliced by rows according to bounding boxes
372 drawn by curators. The row sliced images and the full page images were provided to a third-party
373 curation service, who transcribed the chemical names as SMILES and corresponding assay results.
374 Post-processing analysis and evaluation of a random sample of 150 entries suggest an error rate of
375 <5% in the chemical structures. The final dataset resulted in 18,886 data points on 14,187 molecules.
376 This includes the results on two assay setups, one testing the effectiveness of the candidates on cloth,
377 the other on human skin, and also two different mosquito species (*Aedes aegypti* and *Anopheles*
378 *quadrimaculatus*); all four combinations of these two species and conditions were used in this study.
379 USDA dataset labels in the source material were repellency ratings given as integers from 1 (worst)
380 to 5 (best).⁴¹

381 **A.4 USDA Dataset Modeling and Representation Learning**

382 Each of the USDA tasks was split into a 70:15:15 train/validation/test split such that molecules were
383 assigned to the same split across all tasks; in particular, if a molecule is in the training set for one task,
384 it was also in the training split for the other tasks for which there was a measurement. Molecules
385 in the USDA dataset that were also used in the pre-USDA phase (Batches 1-3, see Supplementary
386 Batch notes) were excluded from the USDA training sets. Iterative stratification over the label
387 classes across each task was applied to balance the labels in the training/validation/test splits for
388 each task.

389 Graph neural network models (GNNs) were trained on each of the four mosquito repellent tasks from
390 the USDA dataset. Each model provided predicted probabilities of the class label and combination
391 class labels; specifically, the model predicted the probability of the class label being: [1], [2], [3],
392 [4], [5], [1 OR 3 OR 4 OR 5], [3 OR 4 OR 5], [1 OR 4 OR 5]. AUROC performance on the [3 OR
393 4 OR 5] label objective was used to optimize the models. The graph neural network used message
394 passing layers (MPNN⁴⁴), with a max atom size of 45, 30 atom features, and 6 bond features.
395 Hyperparameter selections were made using the Vizier⁴³ default Bayesian optimization algorithm
396 over 300 trials.

397 The USDA learned representation was constructed from the outputs of the frozen ensemble model
398 of the best 50 models from hyperparameters trained on the USDA dataset. For the last batch of
399 selections, the models used to create the ensemble model ranged in AUROC performance from
400 0.872 to 0.881.

401 **A.5 Model Training on Membrane Feeding Assay Data**

402 To train the models for activity in membrane feeding assays, assay results were binarized: a positive
403 label for repellency activity was defined as >90% at T=2min at 25 $\mu\text{g}/\text{cm}^2$, and >75% for T=120min.
404 For model evaluation and hyperparameter selection, the dataset was split into a 70:30 train/test split,
405 using iterative stratification to balance the label classes. The model trained on the USDA dataset was
406 used to generate specialized representations for the molecules. A two-layer neural network model
407 with 256 nodes was used to predict the binarized activity label given the molecule; the hyperparam-
408 eters of this model were selected with grid search. At inference time, to make predictions on new
409 candidates, the model was retrained using the entire dataset.

410 **A.6 Molecule Selection**

411 We began by filtering molecules listed in the eMolecules catalog – which contains 1 million commer-
412 cially available molecules – for atom composition (C/N/O/S/H only), price (<\$1000 per 10 grams),
413 purity (>95%), and availability (<4 weeks lead time). We utilized a toxicity filter to remove poten-
414 tially harmful molecules, according to a toxicologist-recommended protocol. In this protocol, we
415 classified molecules by their mutagen / Cramer class using ToxTree, calculated their vapor pressure
416 at room temperature, and then compared the likely exposure air volume to OSHA daily exposure
417 limits for the corresponding toxicity class. We removed likely odorless molecules according to
418 water-soluble ($\text{cLogP} < 0$) and nonvolatile (boiling point > 300 C) criteria. We manually removed
419 molecules that were likely to degrade or react under our experimental conditions. After training
420 the assay model, molecules were selected such that they had a prediction score above an f1 opti-
421 mized cutoff score, and then selected such that they had a Tanimoto similarity of <0.8 from other
422 selected molecules and the USDA dataset. A minimum solubility threshold of 10 mg/ml in absolute
423 ethanol was used as a last criterion. Molecules with an ethanol solubility below the threshold were
424 abandoned. Detailed selection criteria for batches are reported in the Supplemental section.

425 **A.7 Author Contributions**

426 JNW, DMA, KMG, ABW curated and digitized the USDA dataset; JNW, BKL performed data clean-
427 ing and spotchecking of the dataset. MV and KJD designed the mosquito assay and tick assay ex-
428 periments; MV, LB, MWV, and RWMH performed the mosquito assay experiments; MV and MWV
429 performed tick assay experiments. JNW designed the models with assistance from BS-L, BKL,
430 and WWQ. JNW, MV, BS-L, RCG performed data analysis. JNW, MV, RCG wrote the manuscript.
431 ABW and KJD conceived the project. All authors contributed to editing the manuscript.

432 **A.8 Acknowledgements**

433 We wish to thank Laura Pelsen-Posthumus for technical assistance in mosquito rearing, and Geert-
434 Jan van Gemert and Pascal Miesen for provision of mosquitoes. We thank Hans Dautel for help with
435 the design of the tick repellency assay. The authors thank Lucy Colwell, James Thompson, Max
436 Bileschi, and David Belanger for critical reading of the manuscript. We also thank Sameer Kulkarni
437 for assistance with OCR processing and Jonathan Brecher for his insights on transcribing structures
438 from historical chemical names. We thank Jeff Riffel, Carlos Ruiz, Ben Adlam, Jasper Snoek, and
439 the Cambridge Brain Research team for giving helpful feedback during our discussions. Some of
440 the figures were created with BioRender.com. We also thank the Bill and Melinda Gates Foundation
441 for their generous support of this work.